INSTITUTE OF PHYSICS PUBLISHING JOURNAL OF MICROMECHANICS AND MICROENGINEERING

J. Micromech. Microeng. **16** (2006) S297–S302 doi:10.1088/0960-1317/16/9/S18

Design considerations and experimental results of a 100 W, 500 000 rpm electrical generator

C Zwyssig and J W Kolar

Power Electronic Systems Laboratory, Swiss Federal Institute of Technology Zurich, Physikstrasse 3, 8092 Zurich, Switzerland

E-mail: zwyssig@lem.ee.ethz.ch

Received 30 January 2006, in final form 9 May 2006
Published 11 August 2006
Online at stacks.iop.org/JMM/16/S297

Abstract

Mesoscale gas turbine generator systems are a promising solution for high energy and power density portable devices. This paper focuses on the design of a 100 W, 500 000 rpm generator suitable for use with a gas turbine. The design procedure selects the suitable machine type and bearing technology, and determines the electromagnetic characteristics. The losses caused by the high frequency operation are minimized by optimizing the winding and the stator core material. The final design is a permanent-magnet machine with a volume of 3 cm^3 and experimental measurements from a test bench are presented.

(Some figures in this article are in colour only in the electronic version)

1. Introduction

The increasing need for high energy density portable power devices has led to intense research and development efforts on mesoscale systems with power outputs up to 100 W [1]. In this power range, traditional batteries are challenged by devices that use fuel since the fuel provides significantly higher chemical energy density.

An especially promising way of converting the energy stored in the fuel into electrical energy is to use gas turbine generator sets. Accordingly, several international research groups are downscaling traditional gas turbines. For example, researchers at the Tohoku University, Japan, are building a 100 W, 870 000 rpm gas turbine [2], and a team at the Stanford University, USA, has demonstrated a compressor/turbine assembly running at 420 000 rpm with a design speed of 800 000 rpm [3]. A turbine designed at K.U. Leuven, Belgium, has an electrical power output of 44 W at a speed of 160 000 rpm when coupled to a low power commercial generator [4].

In contrast to these mesoscale gas turbine projects, the basic setup of the envisaged system in this project has two compressor/turbine stages. A configuration with two shafts has the advantages of a higher possible pressure ratio than with a single shaft system, which improves the overall efficiency of the system. With increased efficiency and fixed total system mass (including fuel) the allowed mass of the machine increases and compensates for the drawback of a more complex system. The goal for the overall system is an electrical power output of 100 W over 10 h in a volume of 1 litre [5].

All power supply systems based on a gas turbine require an electrical system consisting of a high-speed generator/starter, power electronics, a control platform and a form of energy storage to power the starting of the turbine. However, the research so far has mainly concentrated on the turbine design, and very little research effort has occurred on determining the requirements and the design of the electrical system. The generators under investigation so far are mainly very low power and/or low speed axial-flux generators, partially built with MEMS technology [6–8]. Commercially available machines with the appropriate torque rating are built with speeds up to 100 000 rpm [9]. Therefore, this paper focuses on the design and experimental analysis of a high-speed generator with a rated speed of 500 000 rpm and a required electrical power output of 100 W. The main challenges of the generator design are the losses due to the high frequency in the stator core and windings, the bearing technology, the rotor dynamics and a rotor design minimizing mechanical stresses and eccentricity.

The design method starts with the selection of the machine type and the bearing technology. Then, losses in the windings

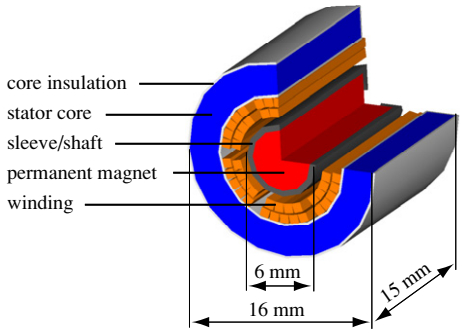

Figure 1. Cross section of the slotless, brushless permanent-magnet generator with slotless winding. The total machine volume is 3 cm^3.

and in the stator core are determined by analytical calculations and minimized. To verify the dimensioning, a test bench setup is realized including mechanical stress analysis and rotor dynamics. Finally, first measurements are presented.

2. Machine selection

A permanent-magnet machine is chosen with the aim of a low system volume, since permanent-magnet flux density remains constant for decreasing machine volume. In contrast, the flux density in an electrically excited motor decreases with decreasing size and is, therefore, not suitable for this application. High-speed operation requires a simple and robust rotor geometry and construction, and excessive mechanical stresses can be limited with a small rotor diameter. Therefore, a radial-flux machine is chosen with a cylindrical permanent magnet encased in a retaining sleeve. A length-to-diameter ratio of 1:1 is defined as this leads to a short shaft which increases the critical speed. The machine designed has an active length of 15 mm and a stator diameter of 16 mm. For highest torque density, high-energy rare earth magnets such as sintered NdFeB or SmCo are the only choices. A Sm_2Co_{17} based magnet is chosen because of its outstanding thermal characteristics (operating temperatures up to 350 °C). A slotless winding is chosen in order to keep the rotor losses low and the stator core manufacturing simple [10]. The peak value of the back EMF is set to 16 V in order to allow the use of low on-resistance power MOSFETs in the power electronic converter. This leads to a phase current of 3 A for the desired power level and a standard three-phase winding. With these benchmark data the electromagnetic machine design is carried out with the help of the finite element software FEMAG [11] for a rated power of 100 W at a speed of 500 000 rpm. A cross section of the machine at the design stage can be seen in figure 1.

3. Bearing selection

For machine speeds in the range of 500 000 rpm, the selection of a suitable bearing is a main issue. In this section, the possible choices are compiled and briefly compared.

High-speed ball bearings are commonly used in the dental industry, and bearings are available for speeds exceeding 500 000 rpm. The main advantages of ball bearings are the robustness and small size. The main disadvantages are the limited operating temperature and a lifetime dependent on lubrication, load and speed.

Static air bearing, dynamic air bearings and foil bearings levitate the rotor with air pressure, either generated with an external supply (static) or by spinning the rotor (dynamic and foil). They all show low friction losses and a long lifetime. Foil bearings are reported for speeds up to 700 000 rpm and temperatures up to 650 °C [12], but are not commercially available and require a complex design procedure.

Magnetic bearings levitate the rotor using magnetic forces and have similar advantages as air bearings. However, active magnetic bearings require sensors, actuators and control, which results in high complexity and increased bearing volume.

In summary, all bearings apart from ball bearings have no wear but just air friction and therefore a long lifetime and low losses. However, due to the simplicity, robustness, small size and avoidance of auxiliary equipment, ball bearings are selected for a first test bench setup. Foil bearings are an interesting alternative, especially for higher operating temperatures, and are considered further.

4. Electrical considerations

The permanent magnet has only two poles in order to keep the fundamental frequency low; nevertheless, the frequency of the currents and the magnetic field in stator winding and core reaches 8.3 kHz at rated speed. This leads to high eddy current and hysteresis losses, which have to be minimized.

4.1. Stator winding losses

Since the stator currents have a fundamental frequency of 8.3 kHz, the losses due to skin effect have to be taken into account. Furthermore, the active part of the winding is exposed to the magnetic field produced by the permanent magnet that rotates with the same frequency. This results in additional eddy current losses. These two losses can be calculated separately and then summed [13]. For a single round wire, the losses caused by the dc resistance and the skin effect are given by (1). The losses caused by the external magnetic field are independent of the current as can be seen from (2). The total losses $P_{tot} = P_s + P_p$ have a minimum for a certain diameter because (1) decreases and (2) increases with increasing diameter.

$$P_s = \frac{\hat{I}^2}{2} F \tag{1}$$

$$P_p = H_e^2 G \tag{2}$$

where $\hat{I}$ is the peak current, H_e is the peak magnetic field strength, and the coefficients F and G are dependent on the conductor diameter, length, conductivity and frequency.

By using litz wire the current in each turn is divided into strands rather than flowing in a single conductor. For any number of strands, and a resulting current per strand, there exists an optimal strand diameter. With this optimal diameter, the total copper losses of the generator can be calculated for different numbers of strands (figure 2). With the chosen litz

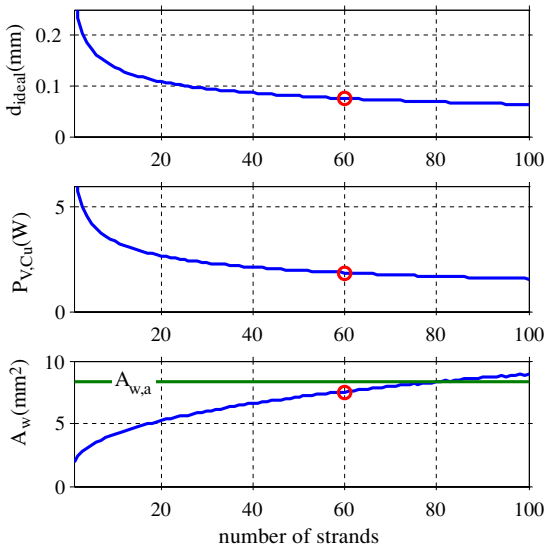

Figure 2. Ideal diameter of one strand (d_{ideal}), total generator copper losses ($P_{V,\text{Cu}}$) and resulting winding area (A_w) versus number of strands. A_w is calculated with a copper filling factor of 0.31. The available winding area is $A_{\text{w,a}} = 8.3$ mm^2. The average magnetic flux in the winding is $B = 0.32$ T at a frequency of 8.3 kHz.

wire of 60 strands and a diameter of 0.071 mm the losses are calculated to be $P_{V,\text{Cu}} = 1.85$ W, which is a 70% reduction compared to using one conductor. The used area including isolation is $A_\text{w} = 7.5$ mm^2, which is still below the available winding area of $A_{\text{w,a}} = 8.3$ mm^2.

4.2. Stator core losses

In the stator core, the magnetic field rotates with high frequency (8.3 kHz) and therefore, a high frequency magnetic material is required. Possible choices are

1. Silicon–iron, 168 μm laminations
2. Amorphous iron-based materials
3. Nanocrystalline iron-based materials
4. Ferrite
5. Nickel–iron, 100 μm laminations
6. Soft magnetic composites.

For sinusoidal induction, the core losses for most magnetic materials can be determined using the Steinmetz equation

$$P_{V,\text{core}} = C_\text{m} \cdot f^\alpha \cdot B_\text{m}^\beta, \tag{3}$$

where C_m, α and β are taken from datasheets. For a first comparison of the materials, the stator core losses are calculated for a frequency of $f = 10$ kHz and a peak magnetic flux density of $B_\text{m} = 0.5$ T (table 1).

Due to the lowest losses and the high Curie temperature, nanocrystalline materials look very promising. However, currently only ring tape cores are manufactured. This is optimal for power inductors and transformers, where the magnetic flux flows along the core. But in the generator the magnetic flux lines enter the core in the radial direction, which results in higher eddy current losses in the vicinity of the entering areas. In high-speed motors for the dental industry, mainly Ni–Fe is used as stator core material. As an example, in a Ni–Fe core with a volume of 1.6 cm^3, a peak flux density of 0.5 T and a frequency of 10 kHz, stator core losses of $P_{V,\text{core}} = 1.2$ W occur.

4.3. Efficiency

Summing up the iron and copper losses the electromechanical efficiency at rated speed and power is calculated to be above 90%. Connected to a power electronics interface the goal for the entire drive system is an efficiency of 80%. Nevertheless, the friction losses (windage and bearing) are expected to outweigh the electromagnetic losses. Depending on the definition of machine efficiency, the friction losses have to be included or not in the total efficiency.

5. Mechanical considerations

In contrast to the usual gluing of the magnets to the shaft, in this machine the retaining sleeve is shrink-fitted onto the permanent magnet and the fully assembled rotor is ground in order to minimize eccentricity without the need of balancing.

5.1. Mechanical stresses

With an interference fit of rotor sleeve and permanent magnet, the stresses on the brittle magnet at high speed are limited. But the stresses in the sleeve are already high at standstill and increase with speed. The stress analysis is carried out analytically according to [14]. The biggest stresses in the whole rotor occur on the inner side of the retaining sleeve. For a titanium alloy sleeve and interference fit of 15 μm, the tangential stress σ_θ becomes 300 N mm^{-2} at standstill and 325 N mm^{-2} at rated speed (figures 3 and 4). With the proper dimensioning of the interference fit the stresses in the magnet can be kept low and the stresses in the sleeve are a sufficient safety margin to the tensile strength of titanium (895 N mm^{-2}). With increasing speed the interference fit loosens due to the

Table 1. Core material properties.

	Density (g cm^{-3})	Curie temp. (°C)	Rel. perm. μ_r	Saturation B_max (T)	Losses[a] (W cm^{-3})
1. Si–Fe	7.6	740	2 000	1.7	3.5
2. Amorphous	7.29	358	<20 000	1.41	0.15
3. Nanocrystalline	7.3	570	<70 000	1.3	0.02
4. Ferrite	4.85	120	<15 000	0.5	0.175
5. Ni–Fe	8.2	310	<80 000	1.48	0.746
6. SMC	3.18	450	<500	2	2.8

[a] Losses at a frequency of 10 kHz and a peak flux density of 0.5 T.

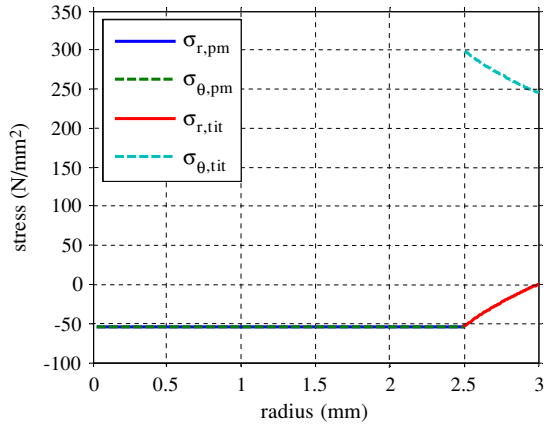

Figure 3. Stresses in Sm_2Co_{17} permanent magnet and titanium sleeve at standstill and a temperature of 23 °C and an interference fit of 15 μm.

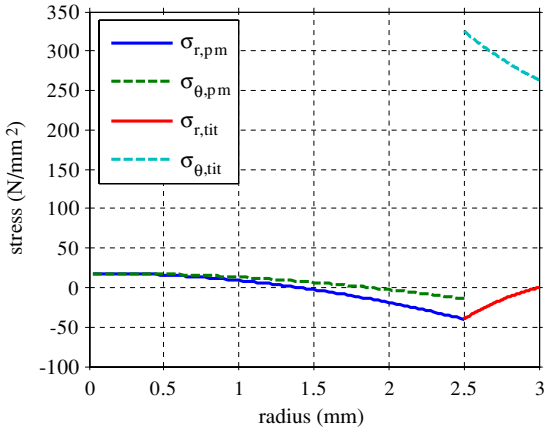

Figure 4. Stresses in Sm_2Co_{17} permanent magnet and titanium sleeve for a speed of 500 000 rpm and a temperature of 23 °C and an interference fit of 15 μm.

Table 2. Bending modes.

Sleeve material	Titanium (Hz)	Steel (Hz)
First bending mode	2400	2300
Second bending mode	4250	3730
Third bending mode	9880	9020

body load. The radial stress ($\sigma_{r,tit} = \sigma_{r,pm}$) must be negative (pressure) over the whole speed range in order to guarantee the torque transfer from the permanent magnet to the retaining sleeve, which also acts as shaft.

5.2. Critical speeds

In order to run the machine in between two critical speeds, the bending modes of the rotor are determined with finite element simulations. The spring constant of the bearing system is taken into account, which shifts the bending modes to lower frequencies. The length of the shaft is adjusted such that rated speed (500 000 rpm, 8333 Hz) falls between the second and the third bending modes (table 2).

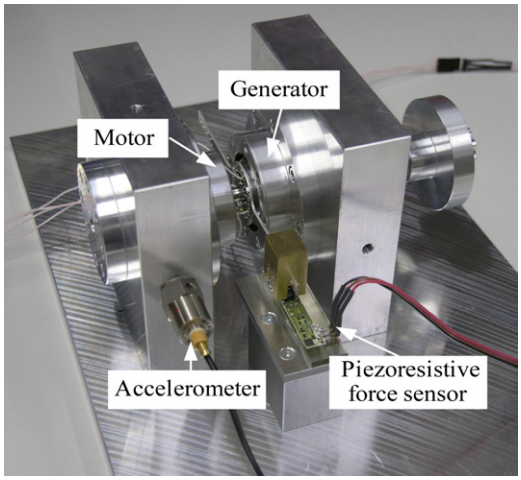

Figure 5. Photograph of the test bench showing motor, generator and sensors.

6. Test bench setup

An experimental test bench is built in order to verify theoretical considerations and the generator concept. Two machines are arranged on a common shaft, one is operated as a driving motor and the other as a generator. The rotor is supported by two radial single row high-speed ball bearings and consists of a titanium retaining sleeve integrating two diametrically magnetized Sm_2Co_{17} permanent magnets, one for the motor and one for the generator. The stator is a ring-wound litz wire around a Ni–Fe core. Figure 5 shows a picture of the test bench setup. The torque is transformed with a moment arm into a force and then measured with a special piezo-resistive sensor (Huba Control Force Cell Type 410).

7. Measurements

With all the parts assembled in the test bench, the theoretical results are verified with initial measurements. The motor is driven open loop with an impressed three phase current of 2.5 A that is of adjustable frequency. For the first tests, an impressed current with a frequency of 8.3 kHz is used to rotate the motor and generator at 500 000 rpm. From the no-load test on the generator side a back EMF of 16 V peak is measured, which matches the value predicted by finite element analysis. As can be seen from figure 6 the back EMF is perfectly sinusoidal. An adjustable resistive three phase load is then connected to the generator side. The generator phase currents are varied between 0 and 2.2 A, the torque is measured and compared to the finite element calculations. Again, there is a very good agreement between predictions and tests (figure 7).

8. Power and control electronics

In order to drive the machine with the rated speed, custom power and control electronics are developed. The very high fundamental frequency, the very low stator inductance and the need for a small and lightweight design presents significant challenges for the power electronics interface.

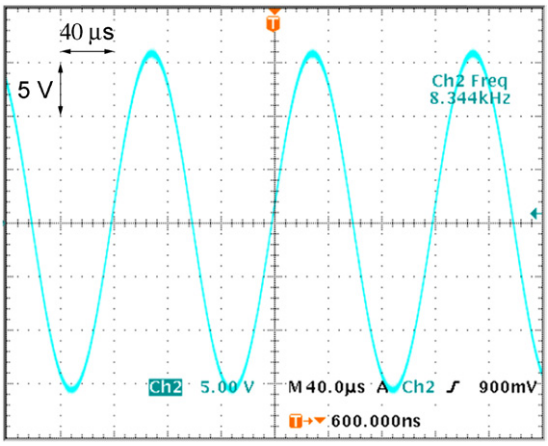

Figure 6. Measured back EMF of the generator in the test bench at 500 000 rpm (40 μs/div, 5 V/div).

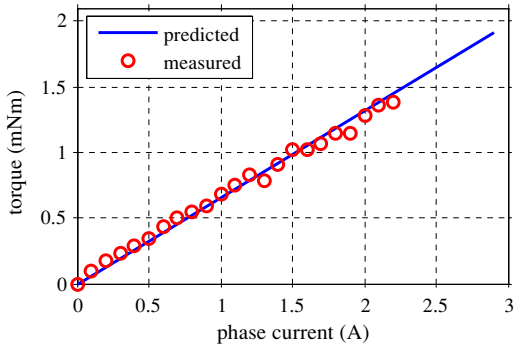

Figure 7. Comparison of predicted and measured torque over phase current.

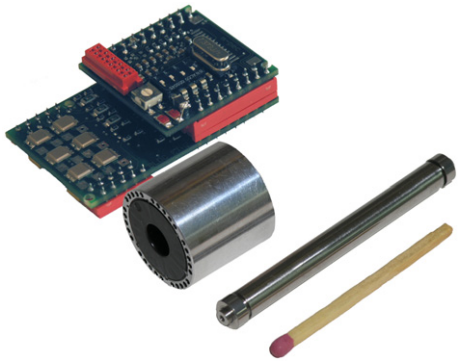

Figure 8. Power and control electronics, stator and rotor of the generator with assembled high-speed ball bearings.

Among several possible topologies three are selected for further investigation and are built in order to evaluate their performance experimentally [15]. The usual voltage source inverter needs external inductances to limit the switching frequency, which still exceeds 100 kHz, and the requirements on current control bandwidth are extremely high. Nevertheless, this topology is the optimal choice with the main focus on size and weight. Considering losses and control complexity, a converter with block commutation, that means that the switching frequency matches the mechanical frequency, becomes attractive. This can either be a current source or a voltage source inverter with additional dc–dc converter at the input for controlling the dc current. The control electronics consist of high-bandwidth analog electronics and a digital signal processor, where sensorless control is implemented.

Figure 8 shows the voltage source inverter with control electronics, the stator and the rotor of the high-speed drive system. It can be seen that even designing the power and control electronics for lowest volume it still has a larger volume than the stator, which demonstrates the need for custom built and integrated electronics. The weight of the stator (25 g) and the electronics (20 g) are also comparable.

9. Conclusion

A high-speed, 100 W, 500 000 rpm permanent magnet generator design for mesoscale gas turbines has been presented in this paper. The losses in the copper winding due to the high frequency currents and magnetic field from the permanent magnet are calculated. The total copper losses are reduced by choosing an appropriate litz wire. To minimize the stator core losses, different magnetic materials are compared and it is shown that amorphous and nanocrystalline materials are the best choices. The rotor is designed with a sufficient safety margin for the mechanical stresses. Titanium is used as a retaining sleeve material in order to limit the stresses on the high-energy Sm_2Co_{17} magnets.

To verify the analytical calculations a test bench has been built, which consists of two machines (one acting as motor and the other as generator) on a common shaft. The critical speeds for the test bench rotor are identified and the length of the shaft is adjusted such that the rated speed falls between the second and the third bending modes. The measurements on the test bench of the back EMF and the torque match the values obtained by finite element simulations very well. Further measurements will be carried out with the custom-built power and control electronics for the motor and generator.

References

[1] Jacobson S A and Epstein A H 2003 An informal survey of power mems *Proc. ISMME2003 (Tsuchiura, Japan, 1–3 December)* pp 513–20

[2] Isomura K, Tanaka S, Murayama M, Yamaguchi H, Ijichi N, Genda T, Saji N, Shiga O, Takahashi K and Esashi M 2003 Development of micro-turbo charger and micro-combustor as feasibility studies of three-dimensional gas turbine at micro-scale *Proc. ASME Turbo Expo, Power for Land, Sea, and Air (Atlanta, GA, USA, 16–19 June)* paper GT2003-38151

[3] Kang S, Johnston J P, Arima T, Matsunaga M, Tsuru H and Prinz F B 2003 Micro-scale radial-flow compressor impeller made of silicon nitride—manufacturing and performance *Proc. ASME Turbo Expo, Power for Land, Sea, and Air (Atlanta, GA, USA, 16–19 June)* paper GT2003-38933

[4] Peirs J, Reynaerts D and Verplaetsen F 2003 Development of an axial microturbine for a portable gas turbine generator *J. Micromech. Microeng.* **13** 190–5

[5] Schneider B, Bruderer M, Dyntar D, Zwyssig C, Diener M, Boulouchos K, Abhari R S, Guzzella L and Kolar J W 2005 Ultra-high-energy-density converter for portable power

Proc. PowerMEMS2005 (Tokyo, Japan, 28–30 November) pp 81–4
[6] Senesky M K and Sanders S R 2004 A millimeter-scale electric generator *Proc. IEEE Industry Applications Conference 2004 (Seattle, WA, USA, 3–7 October)* **1** 346–52
[7] Arnold D P, Zana I, Herrault F, Galle P, Park F W, Das S, Lang J H and Allen M G 2005 Optimization of a microscale, axial-flux, permanent-magnet generator *Proc. PowerMEMS2005 (Tokyo, Japan, 28–30 November)* pp 165–8
[8] Holmes A S, Hong G, Pullen K R and Buffard K R 2004 Axial-flow microturbine with electromagnetic generator: design, CFD simulation, and prototype demonstration *Proc. MEMS 2004 (Maastricht, Netherlands, 25–29 January)* pp 568–71
[9] Kafader U and Schulze J 2004 Similarity relations in electromagnetic motors—limitations and consequences for the design of small dc motors *Proc. ACTUATOR 2004 (Bremen, Germany, 14–16 June)* pp 309–12
[10] Bianchi N, Bolognani S and Luise F 2004 Potentials and limits of high-speed pm motors *IEEE Trans. Ind. Appl.* **40** 1570–8
[11] Reichert K 2004 A simplified approach to permanent magnet motor characteristics determination by finite-element methods *Proc. ICEM2004 (Cracow, Poland, 5–8 September)*
[12] Salehi M, Heshmat H, Walton J F and Tomaszewski M 2004 Operation of a mesoscopic gas turbine simulator at speeds in excess of 700,000 rpm on foil bearings *Proc. ASME Turbo Expo 2004, Power for Land, Sea, and Air (Vienna, Austria, 14–17 June)* paper GT2004-53870
[13] Ferreira J A 1989 *Electromagnetic Modeling of Power Electronic Converters* (Norwell, MA: Kluwer)
[14] Timoshenko S P and Goodier J N 1970 *Theory of Elasticity* (Kogakusha: McGraw-Hill)
[15] Zwyssig C, Round S D and Kolar J W 2006 Power electronics interface for a 100 W, 500 000 rpm gas turbine portable power unit *Proc. Applied Power Electronics Conf. (Dallas, TX, USA, 19–23 March)* pp 283–9